



A Tissue-Penetrating Double Network Restores the Mechanical Properties of Degenerated Articular Cartilage

Benjamin G. Cooper, Rachel C. Stewart, Deborah Burstein, Brian D. Snyder, and Mark W. Grinstaff*

Abstract: Incorporation of an interpenetrating polymer network into an existing single polymer network enables augmentation of the original substrate's mechanical properties, and translation of this concept from purely synthetic materials to natural–synthetic hybrid systems provides the opportunity to reinforce mechanical properties of bulk biological substrates. In many disease states, the mechanical properties of bodily tissues deteriorate rendering them prone to further material failure. Herein, a tissue-supplementing technique is described in which an interpenetrating biomimetic hydrogel is polymerized in situ throughout cartilage tissue. The treatment restores the inferior compressive properties of osteoarthritic cartilage to that of healthy cartilage, preferentially localizing to weaker regions of tissue. Furthermore, the treatment technique preserves cartilage under harsh articulation conditions, showing promise as a materials-based treatment for early-stage osteoarthritis.

The synthesis of polymer double networks, or interpenetrating networks, constitutes a valuable strategy for reinforcing and improving the mechanical properties of one polymer network by physically entangling within it a second network. Several significant strategies have been reported for installing a synthetic interpenetrating network to reinforce synthetic hydrogel networks,^[1,2] biologically inspired polymer networks,^[3] and biomolecule-derived polymer networks.^[4] However, examples of hybrid natural–synthetic double networks, that is, those incorporating a synthetic network within a naturally occurring biopolymer network, are limited to surgical sealants and adhesives.^[5,6] In these reported exam-

ples, the synthetic network forms a physical entrapment and interpenetration only at the tissue surface and not throughout the bulk of the tissue, and therefore such strategies are unable to afford improvement in mechanical properties throughout the tissue.

There are many diseases in which biological tissue undergoes a degenerative weakening process; intervention with a reinforcing tissue-interpenetrating network would be a novel approach to treat or to prevent further tissue damage. Moreover, this strategy has the potential to treat an entire tissue and is in contrast to strategies focused on filling a specific tissue defect or weakened region, as these examples only treat focal lesions and do not remedy widespread degeneration.^[6,7] Osteoarthritis (OA) is one such disease where the depletion of glycosaminoglycans (GAGs), the highly charged polysaccharides responsible for maintaining tissue hydration and imparting healthy cartilage with its high resistance to compression, is a hallmark of the disease.^[8] In a healthy state, the fixed negative charges of the GAGs attract and immobilize water molecules, thereby providing the tissue with significant load-bearing capacity; however as the GAG content of cartilage diminishes over time, so too does its compressive stiffness (Figure 1, left and left-center).^[9] Currently, there are no clinically utilized biochemical or materials-based therapies that either a) mitigate GAG loss, or b) effectively replace lost GAG with a natural or synthetic substitute. We hypothesized that formation of a polymer double network with collagen and a synthetic polymer that bears fixed charges would restore compressive strength to degenerated cartilage by mimicking the GAGs that interpenetrate and attract water via fixed charges in healthy tissue (Figure 1, right-center). Herein, we report the rationale for selecting a phosphorylcholine-based polymer, the synthesis of a semi-natural–semi-synthetic hybrid interpenetrating network with cartilage using in situ photopolymerization, the polymer distribution profile within the tissue, and the assessment of this strategy to reinforce compressive properties and improve cartilage wear resistance.

In such a strategy, small charged monomers first diffuse throughout GAG-deficient cartilage and are then polymerized in situ. Precise chemical mimicry of GAG, with its abundant negative charges, is not optimal as negatively charged monomers equilibrate in lower concentration within the tissue relative to the concentration in surrounding fluid.^[10] Positively charged monomers, in contrast, are electrostatically attracted to diffuse into the tissue,^[11] but many cationic molecules elicit undesirable toxicity.^[12] Therefore, the zwitterionic monomer 2-methacryloyloxyethyl phosphorylcholine (MPC; Figure 1, right), exhibiting no net molecular

[*] B. G. Cooper, Dr. R. C. Stewart, Prof. B. D. Snyder, Prof. M. W. Grinstaff
Departments of Chemistry and Biomedical Engineering
Boston University
Boston, MA 02215 (USA)
E-mail: mgrin@bu.edu
Homepage: <http://people.bu.edu/mgrin>
B. G. Cooper, Dr. R. C. Stewart, Prof. B. D. Snyder
Center for Advanced Orthopaedic Studies, Beth Israel Deaconess Medical Center, Boston, MA 02215 (USA)
Prof. D. Burstein
Department of Radiology, Beth Israel Deaconess Medical Center
Boston, MA 02215 (USA)
Prof. B. D. Snyder
Department of Orthopedic Surgery, Boston Children's Hospital
Boston, MA 02215 (USA)

Supporting information and the ORCID identification number(s) for the author(s) of this article can be found under <http://dx.doi.org/10.1002/anie.201511767>.

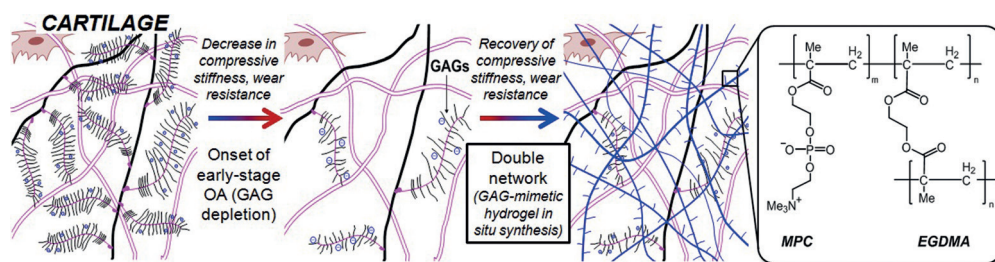


Figure 1. Schematic representation of healthy, osteoarthritic, and hydrogel-reinforced cartilage. GAG depletion during OA decreases cartilage stiffness and wear-resistance; to recover lost properties, a cartilage–hydrogel double network is formed, with stiffness greater than either constituent material alone. Synthetic GAG-mimetic network is composed of hydrophilic zwitterionic monomers (MPC) for hydration and crosslinker (EGDMA) for network formation.

charge yet possessing charged phosphate and trimethylammonium functional groups, was selected as it is known to demonstrate biocompatibility^[13] and a high degree of hydration,^[14] even under extreme compressive loads.^[15]

In a typical treatment procedure, bovine osteochondral explants were either used in their current state (“healthy”) or first enzymatically degraded (“degraded” or “OA”) to selectively decrease cartilage GAG content (see Experimental Section and Supporting Information). Explants were incubated in a solution containing MPC, ethylene glycol dimethacrylate as a crosslinker, and the previously developed^[16] photoinitiating system composed of eosin Y, triethanolamine, and *N*-vinyl pyrrolidone. Explants were removed from solution after a 24-hour incubation, irradiated with green laser light, and rinsed in saline to allow residual non-reacted monomer to wash out. Based on the amount of washed-out monomer as quantified by high-performance liquid chromatography, polymerization efficiency ranged from 70 to 90 % (Figure S1 in the Supporting Information).

Fourier-transform infrared spectroscopy of histological tissue slices after treatment reveals a significant increase in absorbance at 1240 and 1086 cm^{-1} arising from P=O and P–O stretching motions, respectively, attributed to MPC’s phosphate group, and the appearance of a new, strong absorbance at 967 cm^{-1} is indicative of MPC’s trimethylammonium group (Figure S2a). These absorbances are present throughout the superficial, middle, and deep zones of treated tissue (Figure S2b). By incorporation of the fluorescent monomer methacryloyloxyethyl thiocarbamoyl Rhodamine B during the tissue-incubation stage of the treatment procedure, fluorescence microscopy was used to visualize the interpenetrating hydrogel. Figure 2a displays a $10\times$ micrograph (540 nm λ_{ex} , 580 nm λ_{em}), with high fluorescence intensity observed throughout the tissue depth compared to non-treated control tissue. Further verification of the hydrogel’s presence throughout the tissue was obtained by enzymatic tissue digestion of the hydrogel-treated cartilage using papain. As papain cleaves peptide bonds while leaving carbon–carbon bonds (such as those along the MPC polymer backbone) intact, clear MPC hydrogel remained following degradation and dissolution of the cartilage extracellular matrix (Figure 2b).

With this chemical evidence of the polymer’s presence within the treated explants, we sought a translatable and

clinically applicable, non-destructive imaging-based technique for investigating the depth-wise distribution of polymer within the cartilage and the distribution’s dependence on tissue composition at various depths. A degraded explant was imaged by T_2 -weighted magnetic-resonance imaging before and after treatment at a monomer concentration of 60 w/v%

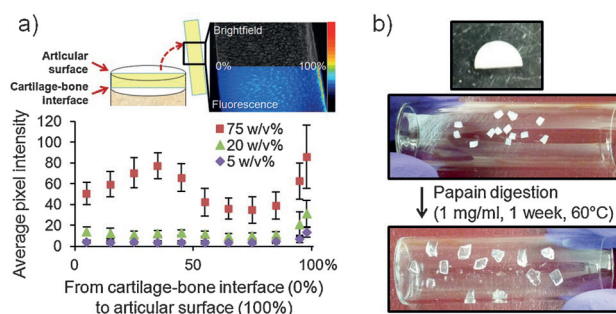


Figure 2. Biochemical characterization of hydrogel presence throughout cartilage. a) By doping the monomer solution with a rhodamine-derived methacrylate monomer, fluorescence microscopy allows visualization of hydrogel-treated tissue (top) and quantification of fluorescence intensity spanning the cartilage–bone interface to the articular surface (bottom). b) A semi-disc (7 mm diameter) of hydrogel-treated cartilage (top) was sliced into small pieces (center) and its extracellular matrix enzymatically digested; clear hydrogel remains (bottom).

(Supporting Information). The average T_2 relaxation time constant over a central coronal slice underwent a statistically significant decrease following treatment, from 52.6 ± 8.6 to 42.3 ± 5.1 ms ($p < 0.001$); this is explained by the hydrogel’s localization in pores of the cartilage previously occupied by water. Since T_2 -weighted imaging is reflective of water volume fraction,^[17] the treatment effectively filled tissue pores with polymer and, thus, the T_2 relaxation time constant decreased (Figure 3a). The concentration of polymer in a region of tissue is proportional to the change in the T_2 relaxation rate ($1/T_2$). By analyzing the change in $1/T_2$ along the gradient from cartilage–bone interface to articular surface, we observed that tissue regions with higher initial T_2 values (generally weaker tissue) experienced greater increases in $1/T_2$ following a single treatment (Figure 3b,c). This finding corroborates the results from the IR study and indicates that the distribution of polymer in treated cartilage is dependent upon the initial tissue composition, in that regions of greater water volume fraction (correlating with mechanically weaker tissue) receive more of the tissue-supplementing material.

Hypothesizing that this “smart” self-distribution of the GAG-inspired hydrogel throughout cartilage will improve

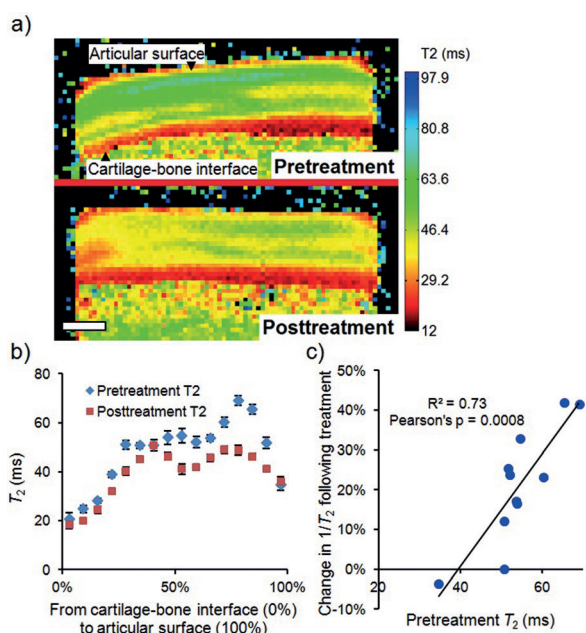


Figure 3. T_2 -weighted MRI of an osteochondral explant before and after hydrogel treatment indicates hydrogel distribution. a) Cartilage T_2 maps (coronal view) before and after hydrogel treatment, with T_2 values averaged over the entire cartilage decreasing from 52.6 ± 8.6 to 42.3 ± 5.1 ms; scale bar, 1 mm. b) Average T_2 as a function of distance from the cartilage–bone interface to the articular surface. c) The strong, statistically significant correlation between pretreatment T_2 and change in $1/T_2$ following treatment suggests that the hydrogel preferentially localizes to tissue regions of most porosity (i.e., those with higher pretreatment T_2 values), thus causing a greater increase in $1/T_2$ in those regions as a result of the hydrogel network occupying tissue pores.

compressive properties, we treated healthy and degraded osteochondral explants (20) as described above using monomer concentrations of 20, 40, and 60 w/v %. Pre-treatment and post-treatment unconfined compression testing was performed and equilibrium compressive modulus (E) was computed (Supporting Information). Healthy explants treated with a monomer concentration of 20 w/v % underwent an average increase in E from 0.31 ± 0.02 to 0.41 ± 0.04 MPa, while degraded explants treated at the same concentration increased from 0.22 ± 0.01 to 0.40 ± 0.01 MPa, corresponding to statistically significantly different ($p = 0.031$ and $p = 0.007$, respectively) increases in modulus of $32\% \pm 10\%$ and $80\% \pm 15\%$, respectively (Figure 4a). The greater percent increase in E associated with degraded tissue state compared to healthy state is rationalized by a greater hydrogel volume filling fraction; as GAGs are enzymatically cleared from cartilage during OA, porosity increases and the cartilage's water content increases,^[18] allowing a greater hydrogel filling volume. A similar trend was observed at increased treatment concentrations, and greater monomer concentrations correlated with greater absolute and relative increases in E (Figure 4). Treatment concentrations greater than 60 w/v % were not investigated as this would likely afford a supraphysiologic articular cartilage compressive moduli. E values reported for human articular cartilage of

the knee range between 0.3–0.8 MPa.^[9,20] Likewise, MPC hydrogels, in the absence of cartilage, became stiffer at increasing concentrations (20 w/v %, liquid; 40 w/v %, $E < 0.001$ Pa; 60 w/v %, $E = 0.0081 \pm 0.0042$ Pa; Figure S3) similar to other reported MPC hydrogels.^[19]

Following demonstration of cartilage mechanical reinforcement at equilibrium conditions, we evaluated the hydrogel's ability to prevent wear, as chondroprotective treatments are of significant interest. Explants (native cartilage or cartilage treated with interpenetrating hydrogel at a monomer concentration of 20 or 60 w/v %, $n = 3$ each) were subjected to a torsional wear procedure under constant compressive stress against polished stainless steel to simulate harsh articulation conditions. The instantaneous tissue thickness was measured over time, and the thickness of the explants upon re-equilibration in saline following up to three sequential procedures was determined by computed tomography (Experimental Section and Supporting Information). The steel countersurface used in this study was intended to cause supraphysiologic shear stresses to simulate accelerated wear.

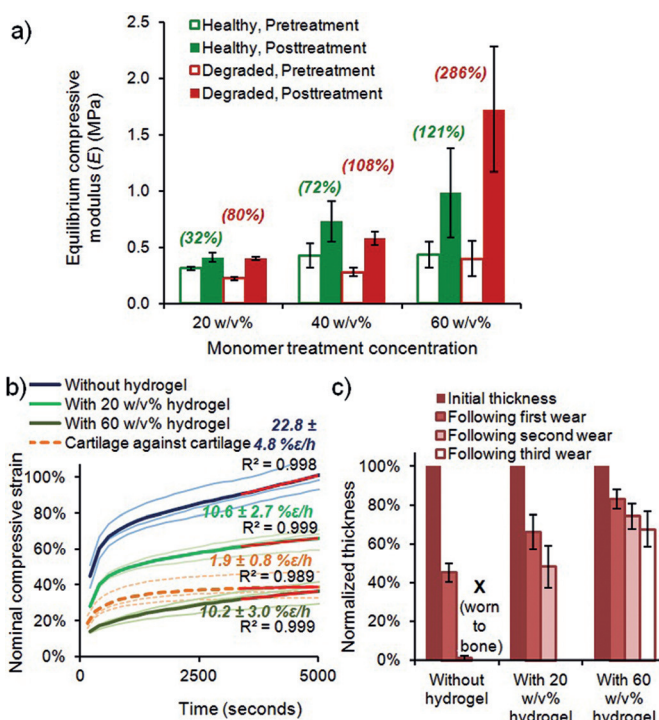


Figure 4. Interpenetrating hydrogel increases cartilage compressive modulus (E), and attenuates creep and reduces wear following repeated articulation. a) Increase in E (relative and absolute) is positively associated with monomer concentration, and degraded tissue underwent greater E increase than healthy control tissue. Average E increase in parentheses; $n = 3$ –4 each group. b) Compressive creep strain as a function of time for cartilage alone and hydrogel-treated cartilage over 5000 cycles of articulation against stainless steel. Cartilage articulating against cartilage shown for comparison (dashed orange). Magnitude of curve slopes displayed in bold text, with linear curve fit displayed as red lines. Thick curves, averages; thin curves, individual samples; $n = 3$. c) Thickness of cartilage alone and of hydrogel-treated cartilage following up to three sequential wear regimens. Thickness normalized to initial thickness; $n = 3$.

Compared to non-treated control samples, the samples treated with 20 and 60 w/v % hydrogel experienced statistically significantly less thickness loss at all time points throughout the first procedure and 34% and 63% less thickness loss, respectively, at the procedure's completion (Figure 4b). The time derivative, that is, the slope of the curves shown in Figure 4b (averaged over the final one third of the procedure) represents the rate of change in thickness, shown in units of percent strain (ϵ)/h. The rate of thickness change of hydrogel-treated cartilage (20 and 60 w/v % concentrations) is approximately half that of non-treated cartilage (10.6 ± 2.7 and 10.2 ± 3.0 ϵ /h compared with 22.8 ± 4.8 ϵ /h, respectively; $p = 0.019$ and 0.018 , respectively). For comparison to physiologic non-wear-inducing conditions, an identical cartilage wear procedure against a cartilage countersurface was also performed (Figure 4b, dashed orange curves), yielding a thickness change rate approximately an order of magnitude lower (1.9 ± 0.8 ϵ /h), indicating that under the conditions investigated by this wear procedure, cartilage-on-cartilage contact experiences negligible thickness loss while cartilage against stainless steel experiences a linear thickness loss. Additionally, this linear portion of the thickness change curve, attributed to tissue loss, engages at a roughly 50% earlier time point for non-treated cartilage (ca. 1400 s) compared to hydrogel-treated cartilage (ca. 3100 s for both 20 and 60 w/v % groups; Figure S4), indicating that the interpenetrating network delays the onset of tissue loss during the regimen. Furthermore, despite articulating against stainless steel, the 60 w/v % hydrogel-treated group undergoes a similar strain profile as the group articulating against cartilage (Figure 4b, dark green vs. oranges curves), supporting the treatment's capacity to restore complex compressive performance comparable to healthy tissue.

Native cartilage was completely worn to the bone (0% thickness remaining) following two successive wear procedures, while 20 w/v % hydrogel-treated cartilage maintained 48 ± 11 % of its initial thickness, and 60 w/v % hydrogel-treated cartilage withstood a third wear procedure and maintained 68 ± 9 % of its initial thickness, indicating significant improvements in tissue preservation (Figure 4c). This follows from the rates of thickness change, that is, the wear rates derived from the creep curves in Figure 4b, as the greater wear rate associated with non-treated cartilage results in greater thickness loss. We propose that the interpenetrating network protects cartilage from wear resistance by a variety of physical mechanisms, most significantly: 1) through polymer chain entanglement, the physically entrapped network dissipates shear stress entropically to reduce the stress on the cartilage matrix, akin to other reinforcing double networks,^[1,21] and 2) because the hydrogel is known to strongly immobilize water, cartilage interstitial fluid load support is maintained for a longer duration into the wear procedure compared to non-treated cartilage. It is also plausible that during steady state cartilage wear, that is, while thickness is linearly decreasing, the magnitude of the treated cartilage's interstitial fluid pressure is greater than that of non-treated cartilage, and this may be a significant factor in the ability to resist wear because it allows more load to be borne by the

fluid component of the tissue rather than by the solid component, which directly addresses a pathology commonly implicated in OA.^[22] Studies are ongoing to further characterize the tissue-protective abilities of this system.

In conclusion, the in situ synthesis of synthetic polymer networks interpenetrated with biological tissue is a useful approach for improving biological materials in need of reinforcement. The tissue-reinforcement mechanism reported in this study affords a polymer double network that interpenetrates the entire cartilage tissue and increases the tissue's equilibrium compressive modulus and wear resistance, providing greater magnitude of strengthening to softer tissue areas and demonstrating preservation of cartilage volume following subjection to harsh articulation. Such a strategy holds promise for the development of biomaterials-based therapies that augment the suboptimal mechanical properties of diseased soft tissues.

Experimental Section

Cartilage-hydrogel double network synthesis: Cylindrical bovine osteochondral explants (7 mm diameter) were used in their current state ("healthy") or first enzymatically degraded with chondroitinase ABC (0.1 U mL⁻¹, 24 h; "degraded" or "OA") to selectively decrease cartilage GAG content (please see Supporting Information). Explants were incubated at 25 °C in a solution containing MPC (concentration ranging 5 to 75 w/v %), ethylene glycol dimethacrylate as a crosslinker, and the previously developed^[16] photoinitiating system composed of eosin Y, triethanolamine, and *N*-vinyl pyrrolidone. Explants were removed from solution after a 24-hour incubation, irradiated with visible laser light (514 nm, 500 mW cm⁻²), and rinsed in saline to allow residual non-reacted monomer to wash out.

Torsional disc-on-disc wear procedure: Explants (native cartilage or cartilage treated with interpenetrating hydrogel at a monomer concentration of 20 or 60 w/v %, $n = 3$ each) were subjected to a torsional disc-on-disc unconfining wear procedure against polished stainless steel, immersed in saline, to simulate harsh articulation conditions. The procedure was composed of simultaneous constant compressive stress (0.78 MPa) and torsion (5000 rotations, 360°/s, effective perimeter velocity 22 mm s⁻¹; 10-s lift-offs every 200 s). The instantaneous tissue thickness was measured over time via the stainless steel's creep displacement, and the thickness of the explants upon re-equilibration in saline (after a period of 18 h) following up to three sequential procedure was determined by computed tomography.

Acknowledgements

We gratefully acknowledge Dr. Benjamin Lakin for insightful discussion and the Preclinical MRI Core Facility at Beth Israel Deaconess Medical Center. This research was financially supported in part by Boston University, the National Science Foundation Graduate Research Fellowship Program (DGE-1247312) (B.G.C.), and the Wallace H. Coulter Foundation.

Keywords: biomaterials · cartilage · double networks · mechanical properties · polymers

How to cite: *Angew. Chem. Int. Ed.* **2016**, 55, 4226–4230
Angew. Chem. **2016**, 128, 4298–4302

- [1] J. P. Gong, Y. Katsuyama, T. Kurokawa, Y. Osada, *Adv. Mater.* **2003**, *15*, 1155–1158.
- [2] a) K. Yasuda, J. P. Gong, Y. Katsuyama, A. Nakayama, Y. Tanabe, E. Kondo, M. Ueno, Y. Osada, *Biomaterials* **2005**, *26*, 4468–4475; b) J. Zhang, N. A. Peppas, *Macromolecules* **2000**, *33*, 102–107; c) X. Zhao, *Soft Matter* **2014**, *10*, 672–687; R. Fei, J. T. George, J. Park, M. A. Grunlan, *Soft Matter* **2012**, *8*, 481–487.
- [3] Y. Iwasaki, Y. Aiba, N. Morimoto, N. Nakabayashi, K. Ishihara, *J. Biomed. Mater. Res.* **2000**, *52*, 701–708.
- [4] a) W. G. Liu, C. Deng, C. R. McLaughlin, P. Fagerholm, N. S. Lagali, B. Heyne, J. C. Scaiano, M. A. Watsky, Y. Kato, R. Munger, N. Shinozaki, F. F. Li, M. Griffith, *Biomaterials* **2009**, *30*, 1551–1559; b) V. X. Truong, M. P. Ablett, S. M. Richardson, J. A. Hoyland, A. P. Dove, *J. Am. Chem. Soc.* **2015**, *137*, 1618–1622; c) Y. Lee, H. J. Chung, S. Yeo, C.-H. Ahn, H. Lee, P. B. Messersmith, T. G. Park, *Soft Matter* **2010**, *6*, 977–983; d) I. C. Liao, F. T. Moutos, B. T. Estes, X. Zhao, F. Guilak, *Adv. Funct. Mater.* **2013**, *23*, 5833–5839.
- [5] a) W. R. Ranger, D. Halpin, A. S. Sawhney, M. Lyman, J. Locicero, *Am. Surg.* **1997**, *63*, 788–795; b) P. Macchiarini, J. Wain, S. Almy, P. Darteville, *J. Thorac. Cardiovasc. Surg.* **1999**, *117*, 751–758; c) H. S. Uy, K. R. Kenyon, *J. Cataract Refractive Surg.* **2013**, *39*, 1668–1674; d) A. M. Oelker, M. W. Grinstaff, *J. Mater. Chem.* **2008**, *18*, 2521–2536; e) C. Ghobril, M. W. Grinstaff, *Chem. Soc. Rev.* **2015**, *44*, 1820–1835.
- [6] D.-A. Wang, S. Varghese, B. Sharma, I. Strehin, S. Fermanian, J. Gorham, D. H. Fairbrother, B. Cascio, J. H. Elisseeff, *Nat. Mater.* **2007**, *6*, 385–392.
- [7] a) K. L. Spiller, S. A. Maher, A. M. Lowman, *Tissue Eng. Part B* **2011**, *17*, 281–299; b) M. K. McHale, L. A. Setton, A. Chilkoti, *Tissue Eng.* **2005**, *11*, 1768–1779; c) D. L. Nettles, T. P. Vail, M. T. Morgan, M. W. Grinstaff, L. A. Setton, *Ann. Biomed. Eng.* **2004**, *32*, 391–397; d) J. K. F. Suh, H. W. T. Matthew, *Biomaterials* **2000**, *21*, 2589–2598; e) K. Yasuda, N. Kitamura, J. P. Gong, K. Arakaki, H. J. Kwon, S. Onodera, Y. M. Chen, T. Kurokawa, F. Kanaya, Y. Ohmiya, Y. Osada, *Macromol. Biosci.* **2009**, *9*, 307–316.
- [8] a) D. T. Felson, R. C. Lawrence, P. A. Dieppe, R. Hirsch, C. G. Helmick, J. M. Jordan, R. S. Kington, N. E. Lane, M. C. Nevitt, Y. Zhang, M. Sowers, T. McAlindon, T. D. Spector, A. R. Poole, S. Z. Yanovski, G. Ateshian, L. Sharma, J. A. Buckwalter, K. D. Brandt, J. F. Fries, *Ann. Intern. Med.* **2000**, *133*, 635–646; b) A. Maroudas, *Nature* **1976**, *260*, 808–809.
- [9] K. A. Athanasiou, M. P. Rosenwasser, J. A. Buckwalter, T. I. Malinin, V. C. Mow, *J. Orthop. Res.* **1991**, *9*, 330–340.
- [10] a) T. S. Silvest, J. S. Jurvelin, M. J. Lammi, J. Toyras, *Osteoarthr. Cartil.* **2009**, *17*, 26–32; b) A. Bashir, M. L. Gray, R. D. Boutin, D. Burstein, *Radiology* **1997**, *205*, 551–558; c) D. Burstein, M. L. Gray, A. L. Hartman, R. Gipe, B. D. Foy, *J. Orthop. Res.* **1993**, *11*, 465–478.
- [11] a) N. S. Joshi, P. N. Bansal, R. C. Stewart, B. D. Snyder, M. W. Grinstaff, *J. Am. Chem. Soc.* **2009**, *131*, 13234–13235; b) P. N. Bansal, R. C. Stewart, V. Entezari, B. D. Snyder, M. W. Grinstaff, *Osteoarthr. Cartil.* **2011**, *19*, 970–976.
- [12] a) J. S. Mader, D. W. Hoskin, *Expert Opin. Invest. Drugs* **2006**, *15*, 933–946; b) O. Boussif, F. Lezoualch, M. A. Zanta, M. D. Mergny, D. Scherman, B. Demeneix, J. P. Behr, *Proc. Natl. Acad. Sci. USA* **1995**, *92*, 7297–7301.
- [13] a) K. Ishihara, H. Nomura, T. Mihara, K. Kurita, Y. Iwasaki, N. Nakabayashi, *J. Biomed. Mater. Res.* **1998**, *39*, 323–330; b) Y. Iwasaki, K. Ishihara, *Anal. Bioanal. Chem.* **2005**, *381*, 534–546; c) T. Moro, Y. Takatori, K. Ishihara, T. Konno, Y. Takigawa, T. Matsushita, U. I. Chung, K. Nakamura, H. Kawaguchi, *Nat. Mater.* **2004**, *3*, 829–836.
- [14] L. Ma, A. Gaisinskaya-Kipnis, N. Kampf, J. Klein, *Nat. Commun.* **2015**, *6*, 6060.
- [15] a) M. Chen, W. H. Briscoe, S. P. Armes, J. Klein, *Science* **2009**, *323*, 1698–1701; b) M. Chen, W. H. Briscoe, S. P. Armes, H. Cohen, J. Klein, *Eur. Polym. J.* **2011**, *47*, 511–523; c) M. Kobayashi, Y. Terayama, N. Hosaka, M. Kaido, A. Suzuki, N. Yamada, N. Torikai, K. Ishihara, A. Takahara, *Soft Matter* **2007**, *3*, 740–746.
- [16] a) D. C. Neckers, *J. Chem. Educ.* **1987**, *64*, 649–656; b) S. M. Linden, D. C. Neckers, *Photochem. Photobiol.* **1988**, *47*, 543–550; c) C. P. Pathak, A. S. Sawhney, J. A. Hubbell, *J. Am. Chem. Soc.* **1992**, *114*, 8311–8312.
- [17] a) K. B. Lehner, H. P. Rechl, J. K. Gmeinwieser, A. F. Heuck, H. P. Lukas, H. P. Kohl, *Radiology* **1989**, *170*, 495–499; b) T. J. Mosher, B. J. Dardzinski, *Semin. Musculoskel. R.* **2004**, *8*, 355–368.
- [18] a) F. Guilak, A. Ratcliffe, N. Lane, M. P. Rosenwasser, V. C. Mow, *J. Orthop. Res.* **1994**, *12*, 474–484; b) H. J. Mankin, A. Z. Thrasher, *J. Bone Jt. Surg. Am. Vol.* **1975**, *57*, 76–80; c) T. Aigner, L. McKenna, *Cell. Mol. Life Sci.* **2002**, *59*, 5–18.
- [19] a) K. Nam, T. Kimura, A. Kishida, *Biomaterials* **2007**, *28*, 1–8; b) K. Nam, T. Kimura, S. Funamoto, A. Kishida, *Acta Biomater.* **2010**, *6*, 403–408.
- [20] a) V. C. Mow, D. C. Fithian, M. A. Kelly, *Articular Cartilage and Knee Joint Function: Basic Science and Arthroscopy* **1990**, 1–18; b) R. K. Korhonen, M. S. Laasanen, J. Toyras, J. Rieppo, J. Hirvonen, H. J. Helminen, J. S. Jurvelin, *J. Biomech. Eng.* **2002**, *35*, 903–909; c) V. C. Mow, R. Huiskes, *Basic Orthopaedic Biomechanics and Mechanobiology*, 3rd ed., Lippincott Williams & Wilkins, Philadelphia, **2005**.
- [21] a) D. Myung, W. Koh, J. Ko, Y. Hu, M. Carrasco, J. Noolandi, C. N. Ta, C. W. Frank, *Polymer* **2007**, *48*, 5376–5387; b) H. Tsukeshiba, M. Huang, Y. H. Na, T. Kurokawa, R. Kuwabara, Y. Tanaka, H. Furukawa, Y. Osada, J. P. Gong, *J. Phys. Chem. B* **2005**, *109*, 16304–16309.
- [22] a) H. Forster, J. Fisher, *Proc. Inst. Mech. Eng. Part H* **1999**, *213*, 329–345; b) G. A. Ateshian, *J. Biomech. Eng.* **2009**, *42*, 1163–1176; c) M. A. Accardi, D. Dini, P. M. Cann, *Tribol. Int.* **2011**, *44*, 565–578.

Received: December 19, 2015

Revised: January 28, 2016

Published online: March 2, 2016